

## Experimental and theoretical studies on the acetaldehyde reaction with (+)-catechin

Raffaele Cucciniello<sup>a</sup>, Michele Tomasini<sup>a,b</sup>, Anna Russo<sup>a</sup>, Laura Falivene<sup>a,\*</sup>, Angelita Gambuti<sup>c</sup>, Martino Forino<sup>c</sup>

<sup>a</sup> Department of Chemistry and Biology 'Adolfo Zambelli', University of Salerno, Via Giovanni Paolo II, 132, Fisciano, Province of Salerno 84084, Italy

<sup>b</sup> Institut de Química Computacional i Catalisi and Departament de Química, Universitat de Girona, c/Maria Aurèlia Capmany 69, Girona, Catalonia 17003, Spain

<sup>c</sup> Department of Agricultural Sciences, Section of Vine and Wine Sciences, University of Napoli 'Federico II', Viale Italia, Avellino 83100, Italy

### ARTICLE INFO

#### Keywords:

(+)-catechin  
Acetaldehyde  
Browning  
DFT calculations  
Vinyl-catechin

### ABSTRACT

Acetaldehyde plays a key role in determining some wine properties. Interesting is the reaction of acetaldehyde with flavonoids, as the ensuing products can alter wine color, astringency, colloidal stability. Many studies reported on the formation of ethylidene-bridged flavan-3-ols as products of the reaction between acetaldehyde and either (+)-catechin or (-)-epicatechin. In white wines after one year of incubation with acetaldehyde only vinyl-(+)-catechin and vinyl(-)-epicatechin were observed, while no ethylidene linked oligomers were detected. This observation prompted us to study the reaction of (+)-catechin with acetaldehyde in wine model solution through an experimental and theoretical approach, with the purpose of exploring the nature of the species involved along with the mechanisms leading to them. The products of the reaction were observed over 38 days. The results showed that ethylidene-bridged catechins are the first products to be formed but over time the dissociation of these dimers causes vinyl-catechins to accumulate.

### 1. Introduction

Reactions of acetaldehyde with flavonoids are of great interest to the enological sector, as they affect sensory properties of wines, such as color, taste and colloidal stability especially during storage and aging (Fulcrand, dos Santos, Sarni-Manchado, Cheynier, & Favre-Bonvin, 1996; Sarni-Manchado, Fulcrand, Souquet, Cheynier, & Moutounet, 1996; Singleton, 1992). In wines, acetaldehyde is produced by yeasts, as a side product of the alcoholic fermentation, but it can also derive from the oxidation of ethanol over time. More specifically, during the first phases of fermentation acetaldehyde is produced and consumed by yeasts to be converted into ethanol to regenerate  $\text{NAD}^+$  from NADH. Only under micro-oxygenation procedures oxygen precludes the conversion of acetaldehyde into ethanol; in these cases, high concentrations of acetaldehyde can be detected (Ji, Henschen, Nguyen, Ma, & Waterhouse, 2020). On account of its volatility and odor activity with a threshold hovering around  $100 \text{ mg L}^{-1}$ , acetaldehyde confers odor notes of grass, bruised apple and nuts (Peynaud & Blouin, 1996). Still, at

higher concentrations it becomes detrimental to the wine quality. As recently shown by Arias-Pérez, Sáenz-Navajas, De-La-Fuente-Blanco, Ferreira, and Escudero (2021), acetaldehyde plays an outstanding role in the modulation of wine aroma as well as of tactile nasal characteristics such as the pungent character. The authors demonstrated that acetaldehyde, at low levels, can play positive roles in some specific aromatic contexts contributing to fruity notes; but, at higher levels, it enhances the negative effects associated to the generic presence of other aldehydes (saturated, unsaturated and Strecker aldehydes) by boosting "green vegetable" notes, "itching" characters, and the "burning" effects linked to high levels of isoamyl alcohol (Arias-Pérez et al., 2021). In wines, acetaldehyde can react with either electrophiles at its alpha position or nucleophiles at its carbonyl functionality. As mentioned above, among natural wine nucleophiles that react with aldehydes, flavonoids such as anthocyanins and flavanols, including (+)-catechin and (-)-epicatechin, play a preeminent role. When acetaldehyde reacts with flavonoids the wine color and its mouthfeel in terms of astringency turn out to be significantly altered (Sheridan & Elias, 2015). It is not easy to

**Abbreviations:** LC-MS/MS, Liquid Chromatography-Mass Spectrometry/Mass Spectrometry; DFT, Density Functional Theory; HPLC, High Pressure Liquid Chromatograph; DNPH, 2,4-Dinitrophenylhydrazine; DAD, Diode Array Detector; LOQ, Limit of quantification; LOD, Limit of detection; LC-HR ESIMS, Liquid chromatography-high resolution-electrospray ionization mass spectrometry; ARP, Acetaldehyde Reactive Potential.

\* Corresponding author.

E-mail address: [lafalivene@unisa.it](mailto:lafalivene@unisa.it) (L. Falivene).

<https://doi.org/10.1016/j.foodchem.2023.136556>

Received 15 January 2023; Received in revised form 28 May 2023; Accepted 4 June 2023

Available online 8 June 2023

0308-8146/© 2023 The Authors. Published by Elsevier Ltd. This is an open access article under the CC BY license (<http://creativecommons.org/licenses/by/4.0/>).

determine when such reactions take place in wines, even though it cannot be ruled out that they likely start already during fermentation. However, apart from the case of micro-oxygenated wines in presence of yeasts (Ji et al., 2020), the reactions between acetaldehyde and flavonoids mostly occur after fermentation, especially if the  $\text{SO}_2$  levels are in a slight molar excess compared to acetaldehyde (Sheridan & Elias, 2016). This specifically applies to wines subjected to prolonged aging. Also, the fate of acetaldehyde is different in white and red wines. In fact, in red wines the occurrence of anthocyanins gives rise to additional acetaldehyde-driven reaction products. It has been proven that in wine model solution acetaldehyde reacts more quickly with flavanols because of their better nucleophilicity at the 8 and, to a lesser extent, 6 positions, in comparison with the same anthocyanin positions. It follows that in white wines only the formation of condensed ethylidene-bridged flavanol dimers and oligomers is observed (Fig. 1).

In red wines, in which anthocyanins and flavanols are simultaneously present, as previously stated, the reaction rate of acetaldehyde with anthocyanins is slower than that with flavanols (Sheridan & Elias, 2016). Accordingly, studies conducted in red wine model solutions have highlighted the preferential formation of ethylidene-bridged dimers

involving two flavanol subunits in addition to less abundant dimers constituted by a flavanol subunit and a malvidin-3-*O*-glucoside, the major anthocyanin occurring in red wines. Also, ethylidene-bridged dimers constituted by two anthocyanin subunits along with oligomers constituted by up to four flavanol units or by up to three flavanol units with either one or two malvidin-3-*O*-glucoside moieties in terminal chain positions have been identified (N. E. Es-Safi et al., 1999; Sheridan & Elias, 2016). Additionally, vinyl-flavanols subunits included in oligomeric structures have been characterized (Cruz et al., 2009). However, even if many studies have been carried out in model solutions, the reactivity of acetaldehyde with phenolics in real wines has been poorly investigated. With the purpose of providing insights into the low weight flavonoids chemical response to acetaldehyde, the reaction products of a white and a red wine were studied by means of untargeted LC-MS/MS analysis after one year of incubation with an excess of acetaldehyde (Cucciniello et al., 2021). Consistently with what observed in wine model solutions, in red wines the formation of ethylidene bridged red pigments was predominant. This positively enhanced the color properties of the wine and, consequently, its stabilization over time. Conversely, in white wine vinyl-(+)-catechin and vinyl-(-)-epicatechin

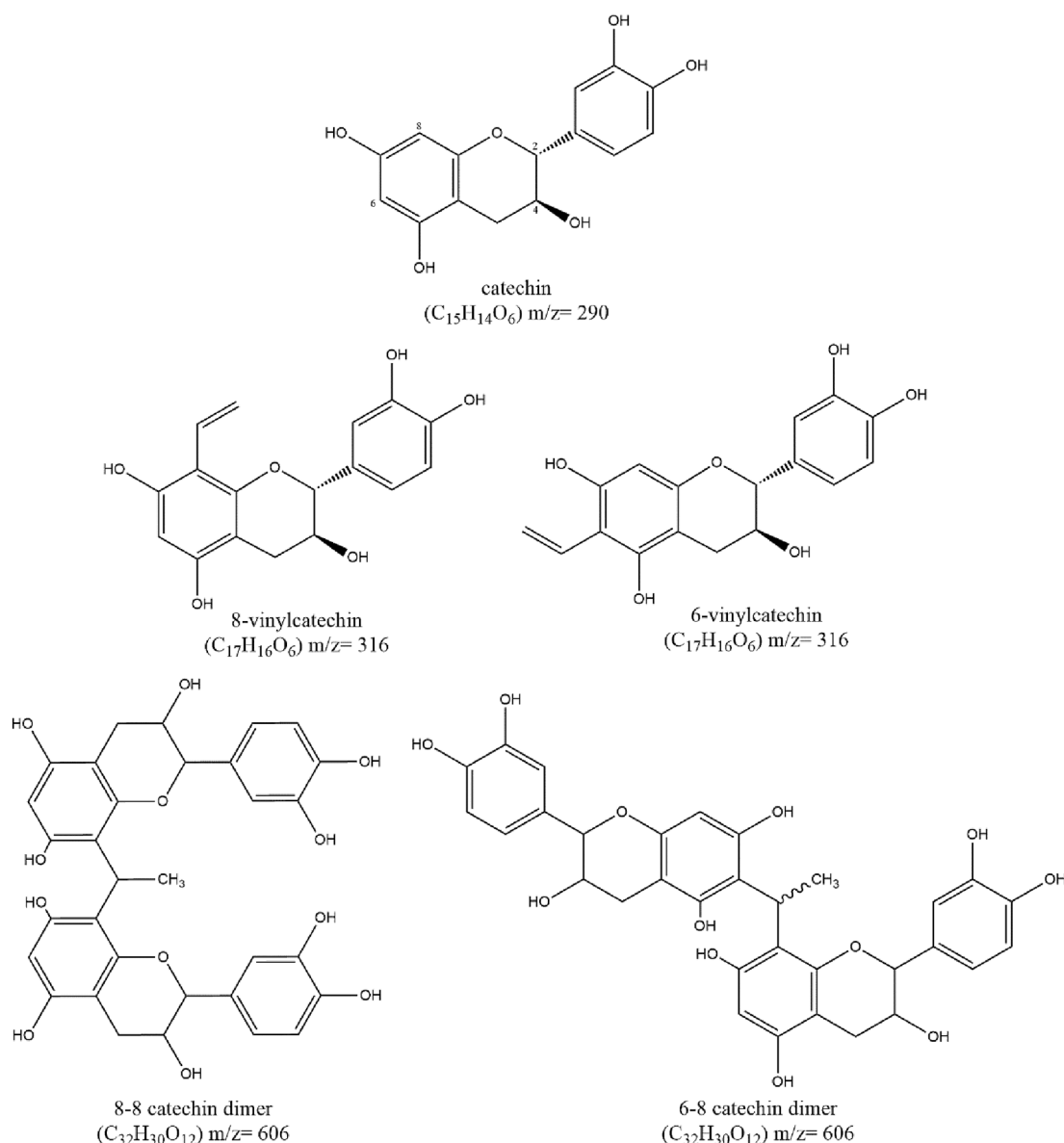


Fig. 1. Chemical structures of (+)-catechin and observed products obtained from the reaction between acetaldehyde and catechin.

monomers emerged as major acetaldehyde-derived compounds, while no ethylidene linked oligomers of flavanols were detected (Cucciniello et al., 2021). Such observation was interpreted as the result of a complex evolution of flavanols mixtures undergoing C–C bond forming and breaking (Dallas, Ricardo-da-Silva, & Laureano, 1996; N.-E. Es-Safi et al., 1999). A double likely origin was proposed for the formation of such vinyl-flavanol adducts. The first hypothesis was that they were formed through a dehydration mechanism undergone by ethyl alcohol-flavan-3-ol adducts initially obtained from the reaction between protonated acetaldehyde and flavan-3-ol at either position 8 or 6 (Guyot, Vercauteren, & Cheynier, 1996). Alternatively, vinyl-adducts of flavanols may be resulting from the depolymerization of the initially formed ethylidene linked flavan-3-ol oligomers.

In this study, we investigated the reaction between (+)-catechin and acetaldehyde in model solution through an experimental and theoretical combined approach. For the first time, a DFT calculation-based approach was adopted, with the ultimate purpose of exploring the reaction mechanisms leading to the complex scenario of products observed experimentally.

## 2. Experimental part

### 2.1. Chemicals and reagents

(+)-catechin (99% HPLC) standards, acetaldehyde (>99.5%), DL-tartaric acid (99%), ethanol, formic acid for LC-MS analysis and acetonitrile (hypergrade for LC-MS LiChrosolv®) were purchased from Sigma-Aldrich (Milan, Italy). Aqueous solutions were prepared with Milli-Q water from Millipore (Bedford, MA, USA). Acetaldehyde, 2,4-dinitrophenylhydrazine (DNPH) and DNPH-acetaldehyde standard were obtained from Sigma-Aldrich (St. Louis, MO, USA). DNPH was purified by recrystallization from acetonitrile.

### 2.2. Preparation of model solutions

Model solutions were prepared in a tartrate buffer containing 5 g L<sup>-1</sup> of tartaric acid, 12% v/v of ethanol, 100 mg L<sup>-1</sup> of (+)-catechin and 40 mg L<sup>-1</sup> of acetaldehyde due to their common concentrations in white wine. The solution pH was brought to 2.0 using HCl 1.0 N. All the solutions were hermetically stored in vials at 25 °C and analyzed at different times over a 38-day stretch of time. Reactions were monitored at pH 2, to increase the kinetic and, thus, to reduce the observation time (Sheridan & Elias, 2016). Experiments were carried out in absence of SO<sub>2</sub> as an antioxidant species, which is generally added to wines to prevent detrimental oxidation reactions. A model solution containing only (+)-catechin (100 mg L<sup>-1</sup>) was used as a control. All experiments were carried out in triplicates.

### 2.3. HPLC-DAD analyses of acetaldehyde

The acetaldehyde concentration was monitored through HPLC-DAD measurements after derivatization in water solution in the presence of DNPH forming DNPH-acetaldehyde (Kim & Pal, 2010). In detail, in a vial, 1.0 mL of sample was treated with 1.5 mL of a 0.13 g L<sup>-1</sup> DNPH in acetonitrile at room temperature and pH 2. Calibration curve was built in the presence of several standard solutions of DNPH-acetaldehyde (0.01 – 40.0 mg L<sup>-1</sup>) prepared by diluting the concentrated standard (1.0 mg mL<sup>-1</sup>) in acetonitrile. Analyses were performed on a HPLC Agilent UltiMate 3000 (Thermo Fisher Scientific, Waltham, MA, USA) equipped with a DAD detector, binary pump, column thermostat and automatic sample injector. Chromatographic separations were carried out by using an Ascentis C18 column (pore size 3 μm × 15 cm × 4.6 mm i.d.) (Supelco, Bellefonte, USA) at 35 °C. A mixture of acetonitrile/water (50/50 v/v) was used as mobile phase at an isocratic flow rate of 0.8 mL min<sup>-1</sup>. The injection volume was 20 μL and the analyses were carried out at 360 nm corresponding to the maximum absorption of DNPH-

acetaldehyde. The limit of quantification (LOQ) was 0.010 mg L<sup>-1</sup> that was the lowest concentration of the calibration curves (linear regression, R<sup>2</sup> > 0.99).

### 2.4. LC-HR-ESIMS analyses

Liquid chromatography-high resolution-electrospray ionization mass spectrometry (LC-HR ESIMS) experiments in the positive and negative ion mode were performed as reported in a previous study (Cucciniello et al., 2021). (+)-catechin standards were used for quantitative determinations by plotting a calibration curve on the basis of peak areas (triplicate injections) at six levels of concentrations (0.1, 0.5, 1.0, 5.0, 10.0, and 20.0 mg L<sup>-1</sup>). (+)-Catechin- and (+)-catechin-derivatives detected in model solution were quantitatively determined by assuming that their molar responses were similar to that of (+)-catechin. The calibration curve equation for (+)-catechin standard was  $y = 0.19232x - 0.0023$  and its linearity was R<sup>2</sup> = 0,9953. LOD and LOQ were 0.36 and 1.09 mg L<sup>-1</sup>, respectively.

### 2.5. Computational details

All DFT calculations were performed with the Gaussian 09 set of programs (Gaussian ~09 Revision D.01 – ScienceOpen, n.d.). The electronic configuration of the molecular systems was described with the hybrid GGA functional of Becke-Lee, Parr, and Yang (B3LYP) (Becke, 1993; Lee, Yang, & Parr, 1988; Stephens, Devlin, Chabalowski, & Frisch, 1994), including dispersion corrections through Grimme's GD3BJ method (Grimme, Antony, Ehrlich, & Krieg, 2010), and using the basis set 6-31G(d) (Ditchfield, Hehre, & Pople, 1971). Solvent effects (H<sub>2</sub>O) were included by using PCM solvation model (Barone & Cossi, 1998; Tomasi & Persico, 1994). The geometry optimizations were performed without symmetry constraints and the characterization of the local stationary points was carried out by analytical frequency calculations. These frequencies were used to calculate unscaled zero-point energies (ZPEs) as well as thermal corrections and entropy effects at 298.15 K and 1 atm. Final energies were calculated through single point calculation at the B3LYP-D3BJ/6-311 + G(d, p) level of theory, with the thermal corrections at the B3LYP-D3BJ/6-31G(d)-PCM(H<sub>2</sub>O) level added to obtain the Gibbs free energies at 298.15 K.

### 2.6. Statistical analysis

To compare the effect of days of treatment on the reaction products formation, analysis of variance (ANOVA) followed by Tukey's test was carried out (p < 0.05). Statistical analysis was performed using XLSTAT 2017 statistical software (Addinsoft, Paris, France). All data are means of three values deriving from three experimental replicates.

## 3. Results and discussion

### 3.1. Reaction of (+)-catechin with acetaldehyde

With the purpose of studying the reaction advancement of (+)-catechin with acetaldehyde, the flavan-3-ol concentration in presence of acetaldehyde was evaluated over a 38-day stretch of time and compared with that of the control model solution. As clearly shown in Fig. 2, the (+)-catechin concentration gradually decreased up to 57 mg L<sup>-1</sup> after 38 days (43% of conversion) consistently with what reported by Sheridan and Elias that after 14 days observed a catechin conversion of 12% at pH 2.0 (Sheridan & Elias, 2016). As discussed in the Experimental part, the reaction with (+)-catechin was investigated at pH 2.0 in order to increase the kinetic while reducing the observation time. In fact, at pH 2.0 the carbonyl acetaldehyde electrophilicity turns out to be increased following its protonation.

In concomitance with the (+)-catechin concentration decrease, the acetaldehyde concentration, due to the compound high reactivity and

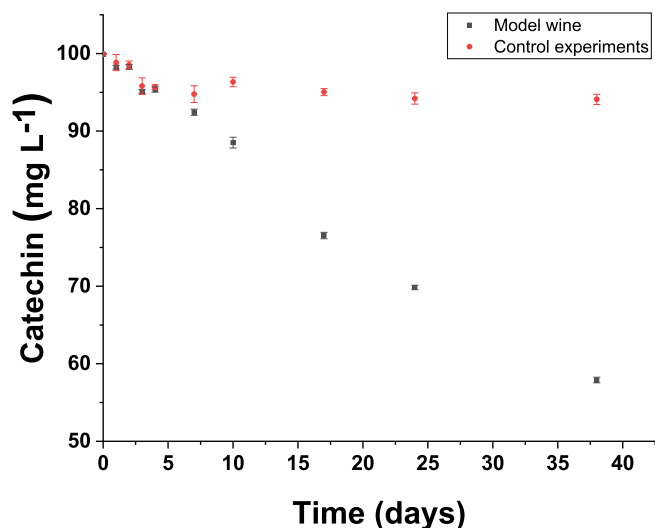


Fig. 2. (+)-catechin concentrations in model solutions (pH 2) added with acetaldehyde (black dots) and in model solutions without acetaldehyde (pH 2) used as a control (red dots). Number of repetitions = 3. (For interpretation of the references to color in this figure legend, the reader is referred to the web version of this article.)

volatility, decreased up to  $1.0 \text{ mg L}^{-1}$  (day 7) to remain constant ( $0.7\text{--}1.0 \text{ mg L}^{-1}$ ) until the end of the experimental observation time (see Table S2).

As expected, the decrease of (+)-catechin in presence of acetaldehyde was due to the formation of condensation products. These latter were identified by LC-HR-ESIMS both qualitatively and quantitatively on the basis of their retention times, HR monoisotopic ion  $m/z$  values, and relative fragmentation ion(s) (Table 1; Fig. 1).

In more details, (+)-catechin was straightforwardly identified by comparison with a pure standard injected under the same experimental conditions. Ion peaks relative to either 6-vinylcatechin or 8-vinylcatechin were assigned on the basis of their relative abundance, which is a consequence of the different reactivity of the acetaldehyde 6- and 8-position towards electrophiles (Drinkine, Glories, & Saucier, 2005). Indeed, the reaction between protonated acetaldehyde and (+)-catechin is regioselective, since the C-8 substitution is sterically favored in comparison to the C-6 substitution. In our experimental settings, two ion peaks at  $m/z$  315 (corresponding to  $\text{C}_{17}\text{H}_{15}\text{O}_6 [\text{M}-\text{H}]^-$ ) emerged at two different retention times, 5.10 min and 5.45 min, respectively. We observed that the ion peak at 5.10 min was the first to appear and its area remained all along higher than that of the ion peak at 5.45 min (Fig. 3). These data led us to assign the ion peak at 5.10 min to 8-vinylcatechin and that at 5.45 min to 6-vinylcatechin. In regards to ethylidene bridged (+)-catechin dimers corresponding to the molecular formula  $\text{C}_{32}\text{H}_{30}\text{O}_{12}$ , four isomers can exist: one 8-8 isomer, one 6-6 isomer, and two 6-8 stereoisomers (Fig. 1). On the basis of the considerations discussed for 6-vinylcatechin and 8-vinylcatechin, throughout

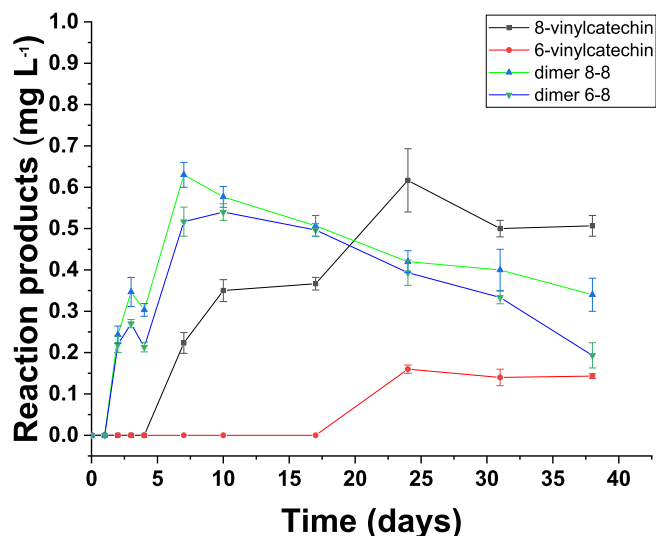


Fig. 3. Products obtained from the reaction between acetaldehyde and (+)-catechin in model wine solutions. Number of repetitions = 3.

the experimental observation time the most abundant ion peak at  $m/z$  605 ( $\text{C}_{32}\text{H}_{29}\text{O}_{12} [\text{M}-\text{H}]^-$ ) was that at 14.10 min followed by another one at 21.68 min. Accordingly, the first peak (14.10 min) was assigned to the most favored 8-8 dimer and the other one (21.68 min) to the 6-8 dimers. The peak at 21.68 min was not as sharp as that at 14.10 min; hence, we assumed that the two 6-8 stereoisomers eluted very close to each other and were not resolved into two separated peaks. Finally, one more ion peak at  $m/z$  605 was detected at 26.11 min and was assigned to the least favored 6-6 dimer. Quantitation of such isomer was not feasible as it was under the quantification limit of our method.

In Fig. 3, the concentrations of the above characterized compounds are displayed (data are also reported in Table S1). As already mentioned, 8-vinylcatechin was observed already after 7 days of incubation with acetaldehyde, whereas 6-vinylcatechin was only detected after 25 days and all along at lower concentrations compared to 8-vinylcatechin. Moreover, the concentration of vinyl-catechins turned out to be stable up to day 38. Conversely, the dimer concentrations (either 8-8 dimer or 6-8 dimers), after an initial increase during the first days (0-7 days), began to decrease after 7 days.

However, it is not to be excluded that, at least, ethylidene bridged (+)-catechin trimers and tetramers could have been formed, but they were not detected under our experimental conditions, as they might precipitate following aggregation and oversaturation of the model solution. It is indeed reported that bridged trimers and tetramers are formed especially when acetaldehyde is in molar excess to catechin, but, once obtained, they tend to aggregate giving rise to the development of haze and some precipitation as well (Peterson & Waterhouse, 2016). If they formed, such oligomers could have been occurring at levels below the limit of detection of our methods and equipment used. This can explain why in our experimental system the observed decrease of

Table 1

LC-HR MS/MS data of the identified products deriving from the reaction between acetaldehyde and (+)-catechin.

Retention time	$[\text{M}-\text{H}]^- m/z$	$\Delta$ (ppm)	Formula	Compound	Fragment ions [MS/MS] ( $m/z$ )
2.72 min	289.0706	-4.018	$\text{C}_{15}\text{H}_{13}\text{O}_6$	(+)-catechin	245, 203, 159, 151, 137, 125, 109
5.10 min	315.0859	-4.797	$\text{C}_{17}\text{H}_{15}\text{O}_6$	8-vinylcatechin	287
5.45 min	315.0861	-4.162	$\text{C}_{17}\text{H}_{15}\text{O}_6$	6-vinylcatechin	287
14.10 min	605.1636	-4.709	$\text{C}_{32}\text{H}_{29}\text{O}_{12}$	ethylidene-bridged (+)-catechin dimer (8-8 isomer)	315, 289
21.68 min	605.1636	-3.882	$\text{C}_{32}\text{H}_{29}\text{O}_{12}$	ethylidene-bridged (+)-catechin dimer (6-8 isomers)	315, 289

(+)-catechin concentration was not quantitatively balanced by the formation of the reaction products.

In order to theoretically substantiate such experimental observations that were consistent with previous reports, we decided to resort to DFT calculations to propose the reaction mechanisms underlying the complex mixture of the observed products.

### 3.2. DFT calculations.

Under acidic reaction conditions, the protonation of acetaldehyde is most likely to occur thus increasing the electrophilicity of its  $sp^2$  carbon that is prone to react with a catechin molecule via Electrophilic Aromatic Substitution ( $s_EAr$ ). The following proton transfer from the *ipso* position of the catechin ring to the oxygen of the 2-hydroxyethyl moiety generates the Wheland-like intermediate (see **Int 2** in Fig. 4) that finally evolves into the formation of a carbocation (see **Int 3** in Fig. 4), thus completing the first pathway under investigation.

In Fig. 4, the complete energy scenario is reported. Our zero-point energy reference is a catechin molecule and a protonated acetaldehyde, coordinated by a water molecule, considered at infinite distance.

Red and black profiles represent the pathways leading to the formation of the carbocation 6 and 8, respectively, obtained by the addition of acetaldehyde to the nucleophilic positions (C-6 and C-8) of the catechin aromatic ring (see labels on the catechin atoms in Fig. 4).

As the acetaldehyde molecule approaches catechin, a hydrogen bond between the catechin hydroxyl group neighboring the electrophilic substitution position on the ring and the water coordinating the acetaldehyde occurs bringing the two molecules together and guiding the addition. After overcoming a kinetic barrier of 7.6 and 9.0 kcal/mol, **8-Int1** and **6-Int1** are formed, respectively ( $\Delta G_{8-Int1} = 3.6$  kcal/mol vs  $\Delta G_{6-Int1} = 5.3$  kcal/mol).

Successively, a water molecule from the solution acts as proton shuttle transferring the proton from the *ipso* position of the aromatic ring to the 2-hydroxyethyl moiety in a concerted way by restoring contemporaneously the ring aromaticity. This proton transfer turns out to be the

rate determining step (rds) of this reaction pathway; and again, it is more favorable for **8-Int1** than for **6-Int1** ( $\Delta G_{6-TS2}^\ddagger = 21.8$  kcal/mol vs  $\Delta G_{8-TS2}^\ddagger = 20.7$  kcal/mol).

It is worth to note that the alternative stepwise mechanism consisting at first in the removal of the *ipso* hydrogen and then in the protonation of the 2-hydroxyethyl moiety from an external water source was ruled out since it is highly unfavored, see SI.

From **Int2**, two water molecules are released into solution with a negligible energy cost (barriers relative to **Int2** of about 5 kcal/mol) leading to the stable carbocations **8-Int3** and **6-Int3** lying about 13 kcal/mol lower in terms of energy with respect to the reactants. Overall, the computational results show that the electrophilic aromatic substitution in position 8 of the catechin ring is kinetically preferred over the substitution in position 6. Looking at the Mulliken charges calculated on C-6 and on C-8 atoms, we observed that C-6 is meaningfully less electron rich than C-8, i.e.  $Q_{C6} = +0.533$  vs  $Q_{C8} = -0.178$  in the catechin,  $Q_{C6} = +0.179$  in 6-TS1 vs  $Q_{C8} = -0.203$  in 8-TS1,  $Q_{C6} = +0.444$  in 6-Int1 vs  $Q_{C8} = +0.071$  in 8-Int1 and  $Q_{C6} = -0.589$  in 6-TS2 vs  $Q_{C8} = -0.738$  in 8-TS2. This difference accounts for the different reactivity of the two carbon atoms with C-8 being more reactive towards the electrophilic aromatic substitution.

Following the formation of the mentioned carbocation, we examined the two mechanisms, E1 (Unimolecular Elimination) and  $s_N1$  (Unimolecular Nucleophilic Substitution) that the carbocation can undergo (see Fig. 5). Starting from the favored carbocation formed in the first pathway, i.e. **8-Int3**, the E1 pathway consists in the deprotonation of the methyl proton by a base yielding the 8-vinylcatechin product (**E-Int6** in Fig. 5). At first, we examined the thermodynamics of this step to determine which molecule among those present in our model solutions, i.e. water, ethanol, or bitartrate, could act as a base strong enough to be involved in such reaction (see Table S3 in SI).

Indeed, we found that only bitartrate can afford the E1 reaction with a favorable thermodynamic scenario. Hence, we investigated the pathway using bitartrate as a base, blue profile in Fig. 5. After the formation of a pre-complex between the base and the carbocation, **E-Int4**,

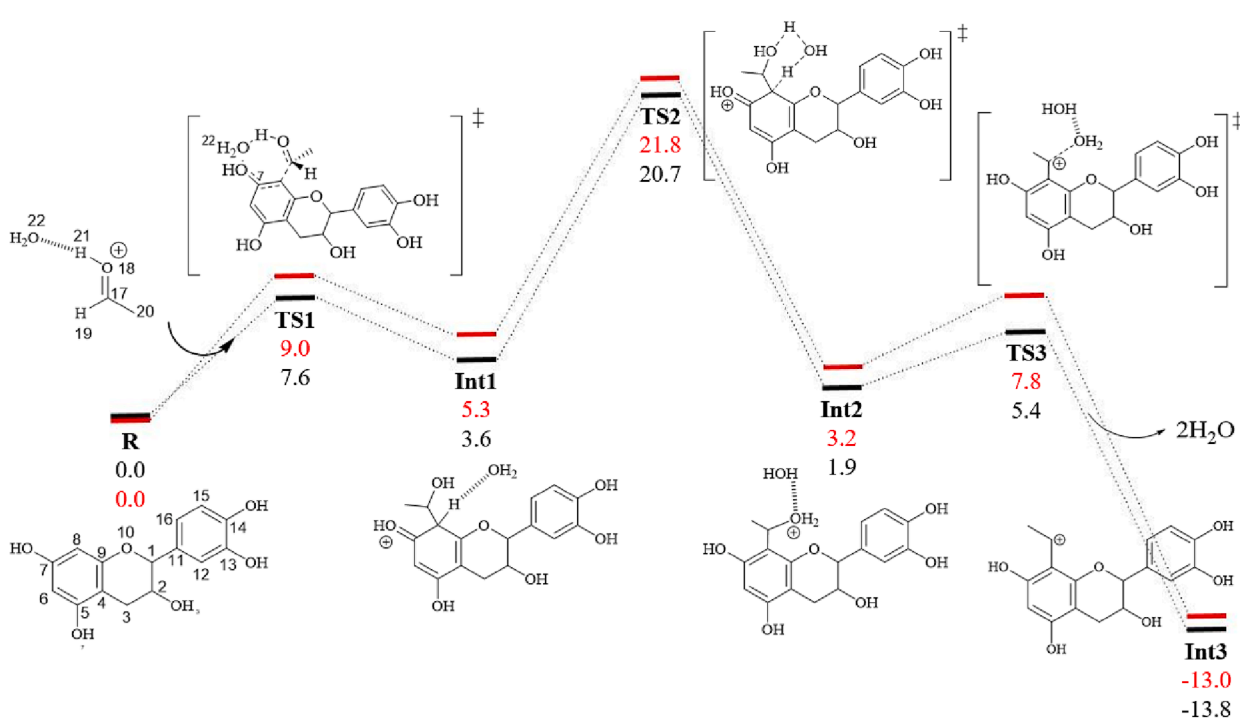


**Fig. 4.** Free energy profile in kcal/mol for the formation of 8-Int3 (in black) and 6-Int3 (in red) and relative structures for 8-Int3 formation. The structures for the other pathway are analogues but the reactive moiety is attached to carbon 6. (For interpretation of the references to color in this figure legend, the reader is referred to the web version of this article.)

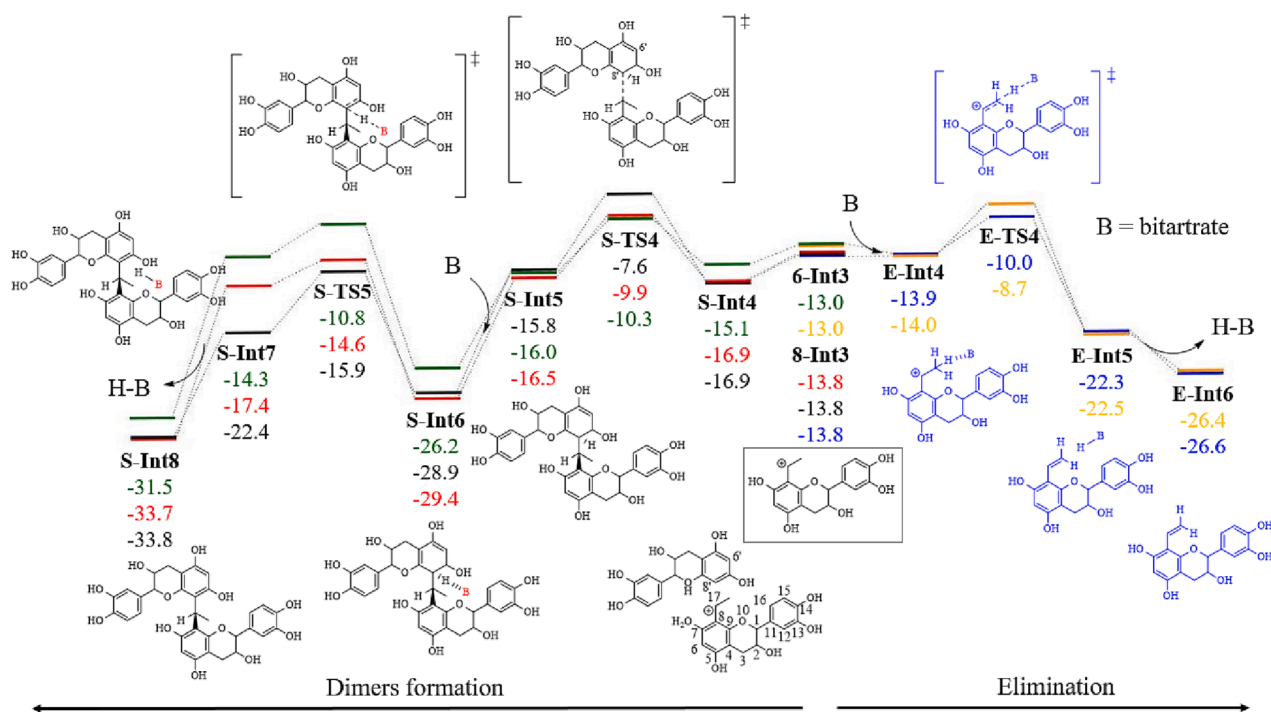


**Fig. 5.** Energy profile in kcal/mol for the formation of dimer 8–8 (in black), 6–8 (in red), 6–6 (in green), 8-vinylcatechin (in blue) and 6-vinylcatechin (in yellow). The drawn structures are referred to 8–8 dimer and 8-vinylcatechin formation. (For interpretation of the references to color in this figure legend, the reader is referred to the web version of this article.)

the deprotonation occurs via **E-TS4** with a relative energy barrier of only 3.9 kcal/mol. The 8-vinylcatechin **Int6** ( $\Delta G_{E-Int6} = -26.6$  kcal/mol) is formed after releasing in solution tartaric acid.

Next, we investigated the  $s_N1$  reaction between **8-Int3** and another catechin molecule forming dimeric structures connected by an ethylidene bridge.

At first, **8-Int3** interacts with the catechin forming a pre-reactant complex **S-Int4** stabilized by 3.1 kcal/mol with respect to **8-Int3** thanks to the formation of a network of hydrogen bonds between the hydroxyl groups of the two moieties. As for the  $s_EAr$  in Fig. 4, the catechin can react in position 6 and in position 8, red and black profiles in Fig. 5, respectively. The reaction requires an energy barrier of 9.3 and 7.0 kcal/mol for **8,8-TS4** and **6,8-TS4**, respectively, at the opposite of the results reported in Fig. 4 for **TS1**. In **8,8-TS4**, the approach of the reactants causes the loss of the hydrogen bonds between the two fragments increasing the energy of the transition state.

Next, as for the E1 mechanism, we investigated which molecule could act as base to efficiently deprotonate the product **S-Int5** leading to the dimeric products observed experimentally (see again Table S3 in SI). Even for this step, only the bitartrate leads to a favorable thermodynamic scenario. After the formation of a pre-reactant complex with the bitartrate stabilized by hydrogen bonds, **8,8-Int7** and **6,8-Int7** ( $\Delta G_{88-Int7} = -22.4$  kcal/mol vs  $\Delta G_{68-Int7} = -17.4$  kcal/mol) are formed overcoming an energy barrier of 13.0 and 14.8 kcal/mol, respectively. In the favored **8,8-TS5** the  $\angle C_5C_8C_{17}$  is  $145.1^\circ$  respect to the analogue  $\angle C_9C_6C_{17}$  of  $126.4^\circ$  in **6,8-TS5** showing that the aromaticity of catechin ring is restored to a greater extent in **8,8-TS5**.

Finally, in Fig. 5 it is also reported in green the energy profile for the formation of the 6–6 dimer obtained from the reaction of the carbocation **6-Int3** with another catechin in position 6 and in yellow the energy profile for the formation of 6-vinylcatechin by E1. Both products were also detected experimentally (Fig. 3).

Looking at the rds of the two new pathways (the elimination for the formation of 6-vinylcatechin **E-Int4**  $\rightarrow$  **E-TS4** and the deprotonation step for 6–6 dimer formation **S-Int6**  $\rightarrow$  **S-TS5**), we can observe that a kinetic barrier of 15.4 kcal/mol must be overcome to form **6,6-Int8**, 2.4 and 0.6

kcal/mol higher than those required to form the 8–8 and 6–8 dimers, respectively, whereas the formation of 6-vinylcatechin requires an energy barrier higher by 1.4 kcal/mol respect to the formation of 8-vinylcatechin.

In summary, the computational results explain the product distribution observed experimentally:

- The 6–6 dimer and the 6-vinylcatechin products require the formation of **6-Int3**, obtained for the reaction of the catechin in the less reactive C-6 position.
- The calculated relative energy barrier for the formation of the dimers increases in the order 8–8 < 6–8 < 6–6 (13.0 vs 14.8 vs 15.4 kcal/mol) and the formation of 6–6 dimer results to be also 2 kcal/mol thermodynamically less stable respect to the other two dimers.
- The energy required for the reverse reaction that leads to the dimer dissociation and back to the formation of the carbocation, i.e. **S-Int6**  $\rightarrow$  **S-Int3**, increases in the order 6–6 < 6–8 < 8–8 (15.9, 19.5, 21.3).
- The accessible dissociation of the dimers accounts for the accumulation over the time of the E1 products since catechin is subtracted from the reaction environment due to the starting  $s_EAr$  reaction.

#### 4. Conclusions

In conclusion, it was theoretically demonstrated that if ethylidene-bridged catechins are the first products to be formed by the reaction between acetaldehyde and (+)-catechin, over time the dissociation of these dimers causes vinylcatechins to accumulate as E1 products. This substantiates previous experimental observations (Cucciniello et al., 2021) that only vinyl-derivatives of flavan-3-ols were present in white wines added with an excess of acetaldehyde after a one-year incubation. The formation of such derivatives is of critical importance to the enological sector. Indeed, it was determined that acetaldehyde is quickly consumed by the reactions with flavanols, whose condensation products evolve into more stable compounds including vinylcatechins. This suggests that an appropriate ratio between acetaldehyde and flavanols could contribute to curb the concentration of free acetaldehyde in wine

and all the detrimental reactions and sensory consequences entwined with free acetaldehyde in wines (Arias-Pérez et al., 2021). In fact, especially in white wines, if not trapped by flavan-3-ols, acetaldehyde may lead to the formation of off-flavor including undesired cyclic acetals and sotolon.

As a future perspective, it would be interesting to investigate the sensory properties of the vinyl-derivatives of flavan-3-ols as to properly evaluate their impact on the quality of the finished wines. Also, taking into account what concluded by Marrufo-Curtido, Ferreira, and Escudero (2022), in order to obtain a more comprehensive picture of the complex acetaldehyde role in wines, it needs to be investigated even the role of factors strategic for wine production such as pH, SO<sub>2</sub> and the content of all the phenolic compounds reactive to acetaldehyde commonly referred to as Acetaldehyde Reactive Potential (ARP). Finally, it is worthy to study even the suitability of bitartrate as a base prompting the E1 reactions that lead to the formation of the vinyl-derivatives.

The ultimate purpose will be to provide insightful pieces of information to enologists in order to develop appropriate viticultural and technological procedures to obtain high-quality wines.

#### CRediT authorship contribution statement

**Raffaele Cucciniello:** Conceptualization, Supervision, Writing – original draft, Resources. **Michele Tomasi:** Methodology, Investigation, Visualization, Formal analysis. **Anna Russo:** Methodology, Investigation, Visualization, Formal analysis. **Laura Falivene:** Writing – review & editing, Conceptualization, Supervision. **Angelita Gambuti:** Software, Writing – review & editing. **Martino Forino:** Writing – review & editing, Resources, Conceptualization, Supervision.

#### Declaration of Competing Interest

The authors declare that they have no known competing financial interests or personal relationships that could have appeared to influence the work reported in this paper.

#### Data availability

Data will be made available on request.

#### Acknowledgement

This work was financially supported by University of Salerno (CTA20CUCCI).

#### Appendix A. Supplementary data

Supplementary data to this article can be found online at <https://doi.org/10.1016/j.foodchem.2023.136556>.

#### References

- Arias-Pérez, I., Sáenz-Navajas, M. P., De-La-Fuente-Blanco, A., Ferreira, V., & Escudero, A. (2021). Insights on the role of acetaldehyde and other aldehydes in the odour and tactile nasal perception of red wine. *Food Chemistry*, 361, Article 130081. <https://doi.org/10.1016/j.foodchem.2021.130081>
- Barone, V., & Cossi, M. (1998). Quantum Calculation of Molecular Energies and Energy Gradients in Solution by a Conductor Solvent Model. *The Journal of Physical Chemistry A*, 102(11), 1995–2001. <https://doi.org/10.1021/jp9716997>
- Becke, A. D. (1993). Density-functional thermochemistry. III. The role of exact exchange. *Journal of Chemical Physics*, 98, 5648–5652. <https://doi.org/10.1063/1.464913>
- Cruz, L., Bras, N. F., Teixeira, N., Fernandes, A., Mateus, N., Ramos, M. J., ... de Freitas, V. (2009). Synthesis and Structural Characterization of Two Diastereoisomers of Vinylcatechin Dimers. *Journal of Agricultural and Food Chemistry*. <https://doi.org/10.1021/jf901608n>
- Cucciniello, R., Forino, M., Picariello, L., Coppola, F., Moio, L., & Gambuti, A. (2021). How acetaldehyde reacts with low molecular weight phenolics in white and red wines. *European Food Research and Technology*, 247(12), 2935–2944. <https://doi.org/10.1007/s00217-021-03841-8>
- Dallas, C., Ricardo-da-Silva, J. M., & Laureano, O. (1996). Products Formed in Model Wine Solutions Involving Anthocyanins, Procyanidin B2, and Acetaldehyde. *Journal of Agricultural and Food Chemistry*, 44(8), 2402–2407. <https://doi.org/10.1021/jf940433j>
- Ditchfield, R., Hefre, W. J., & Pople, J. A. (1971). Self-Consistent Molecular-Orbital Methods. IX. An Extended Gaussian-Type Basis for Molecular-Orbital Studies of Organic Molecules. *Journal of Chemical Physics*, 54, 724–728. <https://doi.org/10.1063/1.1674902>
- Drinkine, J., Glories, Y., & Saucier, C. (2005). (+)-Catechin–aldehyde condensations: Competition between acetaldehyde and glyoxylic acid. *Journal of Agricultural and Food Chemistry*, 53(19), 7552–7558. <https://doi.org/10.1021/jf0504723>
- Fulcrand, H., dos Santos, P.-J.-C., Sarni-Manchado, P., Cheynier, V., & Favre-Bonvin, J. (1996). Structure of new anthocyanin-derived wine pigments. *Journal of the Chemical Society, Perkin Transactions*, 1(7), 735–739. <https://doi.org/10.1039/P19960000735>
- Gaussian –09 Revision D.01 – ScienceOpen. (n.d.). Retrieved January 5, 2023, from <https://www.scienceopen.com/document?vid=839f33cc-9114-4a55-8f1a-3f1520324ef5>.
- Grimme, S., Antony, J., Ehrlich, S., & Krieg, H. (2010). A consistent and accurate ab initio parametrization of density functional dispersion correction (DFT-D) for the 94 elements H-Pu. *The Journal of Chemical Physics*, 132(15), Article 154104. <https://doi.org/10.1063/1.3382344>
- Guyot, S., Vercauteren, J., & Cheynier, V. (1996). Structural determination of colourless and yellow dimers resulting from (+)-catechin coupling catalysed by grape polyphenoloxidase. *Phytochemistry*, 42(5), 1279–1288. [https://doi.org/10.1016/0031-9422\(96\)00127-6](https://doi.org/10.1016/0031-9422(96)00127-6)
- Ji, J., Henschen, C. W., Nguyen, T. H., Ma, L., & Waterhouse, A. L. (2020). Yeasts induce acetaldehyde production in wine micro-oxygenation treatments. *Journal of Agricultural and Food Chemistry*, 68(5), 15216–15227. <https://doi.org/10.1021/acs.jafc.0c06118>
- Kim, K.-H., & Pal, R. (2010). Determination of acetaldehyde in ambient air: Comparison of thermal desorption-GC/FID method with the standard DNPH-HPLC method. *Environmental Monitoring and Assessment*, 161(1), 295–299. <https://doi.org/10.1007/s10661-009-0746-7>
- Lee, C., Yang, W., & Parr, R. G. (1988). Development of the Colle-Salvetti correlation-energy formula into a functional of the electron density. *Physical Review B*, 37(2), 785–789. <https://doi.org/10.1103/PhysRevB.37.785>
- Marrufo-Curtido, A., Ferreira, V., & Escudero, A. (2022). An Index for Wine Acetaldehyde Reactive Potential (ARP) and Some Derived Remarks about the Accumulation of Acetaldehyde during Wine Oxidation. *Foods*, 11(3), 476. <https://doi.org/10.3390/foods11030476>
- Peterson, A. L., & Waterhouse, A. L. (2016). 1H NMR: A Novel Approach To Determining the Thermodynamic Properties of Acetaldehyde Condensation Reactions with Glycerol, (+)-Catechin, and Glutathione in Model Wine. *Journal of Agricultural and Food Chemistry*, 64(36), 6869–6878. <https://doi.org/10.1021/acs.jafc.6b02077>
- Peynaud, E., & Blouin, J. (1996). *The Taste of Wine: The Art Science of Wine Appreciation*. John Wiley & Sons.
- Sarni-Manchado, P., Fulcrand, H., Souquet, J.-M., Cheynier, V., & Moutounet, M. (1996). Stability and Color of Unreported Wine Anthocyanin-derived Pigments. *Journal of Food Science*, 61(5), 938–941. <https://doi.org/10.1111/j.1365-2621.1996.tb10906.x>
- Sheridan, M. K., & Elias, R. J. (2015). Exogenous acetaldehyde as a tool for modulating wine color and astringency during fermentation. *Food Chemistry*, 177, 17–22. <https://doi.org/10.1016/j.foodchem.2014.12.077>
- Sheridan, M. K., & Elias, R. J. (2016). Reaction of Acetaldehyde with Wine Flavonoids in the Presence of Sulfur Dioxide. *Journal of Agricultural and Food Chemistry*, 64(45), 8615–8624. <https://doi.org/10.1021/acs.jafc.6b03565>
- Singleton, V. L. (1992). Wine and Enology: Status and Outlook. *American Journal of Enology and Viticulture*, 43(4), 344–354.
- Stephens, P. J., Devlin, F. J., Chabalowski, C. F., & Frisch, M. J. (1994). Ab Initio Calculation of Vibrational Absorption and Circular Dichroism Spectra Using Density Functional Force Fields. *The Journal of Physical Chemistry*, 98(45), 11623–11627. <https://doi.org/10.1021/j100096a001>
- Tomasi, J., & Persico, M. (1994). Molecular Interactions in Solution: An Overview of Methods Based on Continuous Distributions of the Solvent. *Chemical Reviews*, 94(7), 2027–2094. <https://doi.org/10.1021/cr00031a013>